ACTA IMEKO
ISSN: 2221-870X
September 2023, Volume 12, Number 3, 1 - 9

Problems of software processing of acquired rotor intended for determining required dimensions

Dražen Turinski[1], Ilija Svalina[1], Roberto Lujić[1], Tomislav Šarić[1], Goran Šimunović[1], Sara Havrlišan[1]

[1] *University of Slavonski Brod, Mechanical Engineering Faculty in Slavonski Brod, Slavonski Brod, Croatia*

ABSTRACT
Some of the problems that arise during image processing are analysed in this paper. The most commonly used software tools in image processing require binary photography, and its conversion into the binary form is required first. Conversion problems, and their proper solution, are key steps for further machine determination of product dimensions. Removing smudges on binary photos and rotating displays for photo overlap methods are the problems that are solved in the present work, in order to successfully prepare the photo with software for further determination of product dimensions. The knowledge gained in this paper will help scientists and facilitate their software preparation and processing of the photo used to determine the required dimensions of the product.

Section: RESEARCH PAPER

Keywords: Digital photography; image processing; dimensional acceptability; quality control

Citation: Dražen Turinski, Ilija Svalina, Roberto Lujić, Tomislav Šarić, Goran Šimunović, Sara Havrlišan, Problems of software processing of acquired rotor intended for determining required dimensions, Acta IMEKO, vol. 12, no. 3, article 12, September 2023, identifier: IMEKO-ACTA-12 (2023)-03-12

Section Editor: Marija Cundeva-Blajer, Ss. Cyril and Methodius University in Skopje, North Macedonia

Received January 23, 2023; **In final form** June 28, 2023; **Published** September 2023

Corresponding author: Dražen Turinski, e-mail: dturinski@unisb.hr

1. INTRODUCTION

Software processing of digital photos has a wide range of applications, processing within different software packages and using different methods, in order to use a quality processed photo for the desired purposes. Depending on the field of application, there are problems that researchers face and must be successfully solved in order for the software solution to make sense to be implemented in quality control systems.

A review of the literature will show some of the areas in which software systems have been implemented. The paper [1] presents a developed system in which a programmed algorithm for automatic detection of errors in the production of MPCG (Mobile Phone Cover Glass) is incorporated. In the food industry, in paper [2] photographs acquired by hyperspectral cameras are processed by software and used for automatic detection of errors in the food packaging process. In the field of mechanical engineering, the digital photo obtained during laser welding in paper [3] was processed by software and an algorithm was developed to monitor the accuracy of the product. For the quartz bar industry, by developing quality control, a method for detecting bubbles in quartz bars and evaluating their quality based on machine vision was developed in paper [4]. In all the mentioned works, the key part is the photo processing and their successful solution to the photo processing problem. The problems of photo binarization [5] must be properly solved so that it makes sense to use the photo in the further process. In the following, some of the solutions that the researchers used in their works will be presented. In paper [6] the Sauvola method was applied for adaptive photo binarization, while in paper [7] and [8] the Otsu method was used to solve the problem of binarization. Also, in the paper [8] the problems of removing smudges and rotation of the display were considered. Methods for solving the problem of photo rotation are presented in [9] and [10]. As photo processing has become widely used as a means of reducing detection time and production effort in the paper [11], the study proposes an algorithm for photo processing that solves, among other things, the above-mentioned problems.

By researching the literature, it can be established that the field of application of digital photography is wide and that a large number of problems are encountered during the software processing of photographs. Therefore, the focus of this paper on the problems of software processing of photographs are intended to determine product dimensions.

2. PROBLEM DESCRIPTION AND RESEARCH GOAL

In the introduction, through a brief review of the literature, it was possible to see that the use of photography to determine product dimensions with regard to the required dimension of the product is not widely used in science and industry. The reasons, among other things, lie in the problems that arise on the implemented hardware and software solutions of computer and machine vision. The implemented solution acquires and processes digital photos, which depends on the correctness of product dimensions. Part of the surface of the photo that is not occupied by the product is unusable, it is removed during processing, which reduces the number of pixels in the photo and thus the tolerance limits because there are fewer pixels in the product. Photographs taken in RGB or in shades of grey (greyscale) must be converted into black and white binary form (0 and 1), which is a prerequisite for further processing with the most used software tools. The software loads the photo as a matrix with numbers, where each number in the matrix represents a pixel or a colour of the photo. The problem arises when converting the photo into black and white binary form. Monochromatic photos have only black and white, that is, depending on the resolution of the A/D converter of the acquisition device to which the dynamic range of digital values converts the input voltage, for example, an 8-bit A/D converter converts a voltage of [0, 1 V] into numbers of [0, 255]. This means that the range of light (dynamic range) from black to white is represented in 256 shades of grey. Which means that it is necessary to choose a shade of grey that will be the threshold value of black, and all other shades with a number greater than the threshold value are converted to white. Successful binarization solves an important prerequisite for further software preparation of the photo for the correct determination of the product dimensions. After binarization, smudges may appear on the photo caused by impurities, shadows, noises and other disturbances during photo acquisition or software processing. They can negatively affect the measurement of the properties of the parameters of the observed product region in the photo, which will be further used to determine the product dimensions. Therefore, successful removal of smudges with binarization is an essential prerequisite for further determination of the product dimensions. With software packages, certain tools rotate the photo around its centre, so it is necessary to crop the photo so that the product is exactly in the centre. With the photo overlay method, in determining the dimensional correctness of the product in the photo, it is important to centre the product and orient it correctly so that the method is effective. Therefore, the mentioned problems of centring, cropping and rotation of the product in the photo are analysed in this paper. The goal of this research is to gradually improve the algorithms for the above-mentioned problems of software photo processing, which will provide a quality solution and thus improve and facilitate the software preparation and processing of digital photos intended for determining the required dimensions of the product.

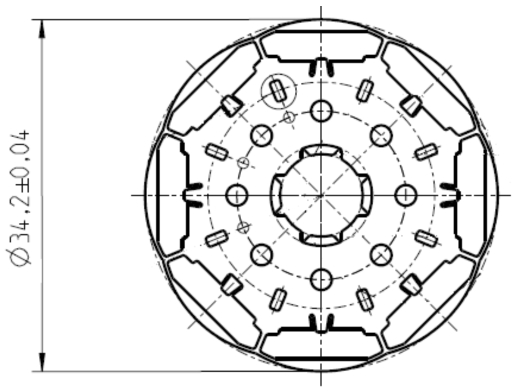

Figure 1. The diameter of the rotor.

Figure 2. Canon camera, lens and illumination.

3. DESCRIPTION OF CONDUCTED EXPERIMENTAL RESEARCH

In this paper the above-mentioned problems that arise during the software processing of the digital photograph will be considered on the acquired digital photograph of the rotor sample. The diameter of the rotor is defined by the technical drawing see Figure 1, the sample of which is used during the first phase of preliminary research for the development of machine vision on the prototype machine for quality control, according to the project financed by the European fund for regional development (project code: KK.01.2.1.02.0062):

For software processing, a digital photography of the sample obtained in a laboratory environment using a Canon EOS 600D digital SLR camera, EF-S 18-55 IS II lens and illumination with a 3M 9700 overhead projector model 9000 AHJS was used, see Figure 2.

Digital photography acquired by Canon camera used for processing is shown on Figure 3.

Within the paper [12], advice and recommendations are given on what features acquisition equipment should have. Based on that, industrial cameras from Allied Vision model Alvium 1800 U-507m were used, bi-telecentric lens from Opto Engineering model TC23085 and the illumination of parallel light radiation

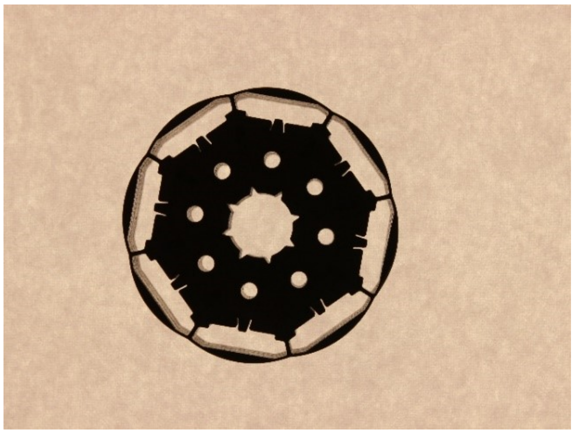

Figure 3. Canon’s photo.

Figure 4. Alvium camera, lens and illumination.

located below the sample from GETCAMERAS model LED 1-FL-83x75 see Figure 4.

Digital photography acquired by Alvium camera used for processing is shown on Figure 5

The digital photographs were processed within three different software packages (Matlab, R studio and FabImage). Already when opening a Canon's photo within the software packages, problems arise caused by the high resolution of the photo, which greatly slows down the use of certain software tools. Since the Canon photo was acquired in colour and Alvium photo in the greyscale, so first both must be converted into a greyscale. This is followed by the binarization of the photo, which was done in Matlab software package using Otsu's method and the Adaptthresh method with an adaptive grey border. R studio software package performed binarization using 11 different methods (Bernsen, Niblack, Sauvola, Wolf, Nick, Gatos, Su, Trsingh, Bataineh, Wan and ISauvola) and FabImage software package by TresholdImage method but only on Alvium's photo. Photos binarization was performed according to the default settings of each individual method within the software package. Due to the problems that arise when connecting tools from different libraries, the binarized photos obtained using the mentioned 11 methods were saved in JPEG format and were analysed and processed in the first software package. For each binarized photo, the number of pixels that make up the surface of the rotor, as well as the number of pixels located on the largest horizontal part of the rotor (width) and on the largest vertical part of the rotor (height) were determined using software tools. As the rotor sample was acquired by equipment whose lens has

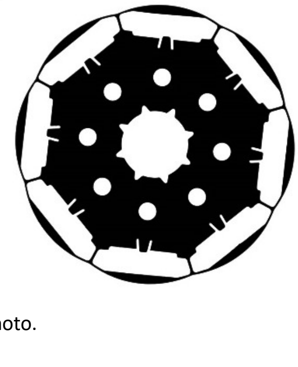

Figure 5. Alvium's photo.

a central projection see Figure 2, in Figure 3 you can see the appearance of the third dimension, which creates smudges on the binarized photos that cause problems and must be removed as well as other smudges caused by impurities on the surface, noises and other errors created upon acquisition and by poor binarization methods. Comparing with Alvium's photo acquired with a bi-telecentric lens, one can visually notice the appearance of significantly less smudges. To solve the mentioned problem, the smudges removal tool was used within the software using the automatic settings of the tool Bwareaopen. The number of pixels removed was then calculated. As with some binarization methods there are smudges that are larger and cannot be removed by the automatic settings of the tool used, by combining different tools available in the used programs ('bwconncomp', 'regionprops', 'labelmatrix', 'ismember'), used within the loop, simple algorithms have been developed to remove smudges, then the total number of removed pixels is calculated.

After that, the total number of pixels in the surface of the rotor after the smudges were removed, and the width and height of the rotor were calculated. Since the number of calculated pixels of the rotor surface differs with the binarization methods used in the obtained photos, a problem arises when choosing a method that gives accurate results, which is also a key prerequisite in determining the dimensional correctness of the rotor. In order to analyse the problem on both processed photos, the mean value of the number of the rotor pixels without smudges from all 14 methods used is calculated. The deviations of all methods are calculated in relation to the mean values. The width and height of the rotor are calculated with the mean value of the number of pixels of the rotor without smudges, and the results obtained with other methods are analysed. With each binarization method, for the obtained value of the number of pixels of the rotor, a software algorithm is used to determine which threshold shade of grey colour during binarization corresponds to the value of the obtained pixel numbers. An algorithm is then programmed so that every pixel with a shade of grey that is less than the smallest threshold shade of grey is converted to black, and every pixel whose shade of grey is greater than the highest threshold shade of grey is converted to white. While all other shades of grey remain unchanged. In this way, the layout of the pixels in the photo can be visually seen, and by calculating the size of the pixels in the processed photo, it can be concluded whether there are dimensional deviations or whether the dimensions of the product are within the tolerance limits. Photographs processed in this way can be used to determine the product dimensions using different methods. With the overlay method, the photo is binarized with a shade of grey according to the above-calculated mean value of the shades of all methods used, and the smudges removed where the photo processed in this way is overlapped over the reference photo and the dimensional correctness of the product is determined. In order to solve the problem, it is necessary to position the product in the same position and the same orientation as the product in the reference photo. Therefore, it is necessary to find the centre of gravity and the centre of the product. The position of the edge pixels of the rotor at the top, bottom, left and right sides was determined by the algorithm of the repeating loop, and thus the centre was calculated. In another way, the edge pixels were determined using a software tool that automatically calculates them, as well as a software tool for determining the centre of gravity of the rotor. With the rotor, in case the smudges are not well removed, the problem arises that the centre of gravity of the product and the centre of the product are not in the same place. When rotating the photo, it is important that the product is in the centre and that the photo has the same width and height. In order to properly prepare the photo, cropping was done according to the required conditions. When rotating a photo, there is a deviation in the number of pixels depending on the angle of rotation. In terms of the number of pixels of the total area, the deviations are not significant, while the problem occurs at the edges of the product where, after rotation, large changes in the arrangement of pixels on the edge can be observed. The analysis of the problem is considered by rotating the photo by half a degree and by one degree. By analysing and researching the above-mentioned problems, the goal is to find an algorithm that will facilitate the software processing of digital photography to determine the required product dimensions.

4. RESULTS OBTAINED

Binarization of the Canon's photo was performed with 13 different methods within 2 different software packages, while Alvium's photo with one more software package (FabImage) that use new method (TresholdImage). Software tools were used to calculate the number of pixels representing the surface of the rotor, as well as the number of pixels in the width and height. The results of the Canon's photo are shown in Table 1, where it can be seen that the Adaptthresh method has an area of 13625262 pixels which is the most, while the Gatos method has the least (828255 pixels). The width and height of the Adaptthresh, Bernsen and Niblack methods differ greatly compared to the other methods.

On the example of a photograph binarized by the Bernsen method in Figure 6a, the reason for the large number of pixels obtained can be seen. Smudges are included in the pixel surface. In the binarized photo using the Nick Figure 6b method, you can see why the rotor surface has significantly fewer pixels than the other methods. It can be seen that a large number of pixels of the rotor surface are not included in the surface area.

The results of binarization for Alvium's photo are shown in Table 2. Again, it can be seen that the Adaptthresh method does

Table 1. Features of the rotor of the Canon's photo.

Binarization methods	Area (pixels)	Width (pixels)	Height (pixels)
Otsu's	2562799	2242	2246
Adaptthresh	13625262	4607	3455
Bernsen	8961137	4607	3455
Niblack	9537052	4607	3455
Sauvola	1113171	2241	2245
Wolf	1318170	2241	2245
Nick	967796	2240	2244
Gatos	828255	2241	2245
Su	1558446	2240	2244
Trsingh	1067834	2241	2244
Bataineh	2660714	2242	2247
Wan	2058419	2243	2246
ISauvola	1108493	2241	2245

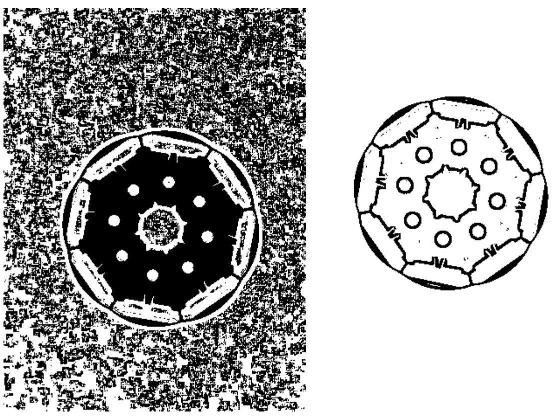

Figure 6. Bernsen method (a) and Nick method (b).

Table 2. Features of the rotor of the Alvium's photo.

Binarization methods	Area (pixels)	Width (pixels)	Height (pixels)
Otsu's	490992	1019	1020
Adaptthresh	1606839	1489	1381
Bernsen	490785	1080	1041
Niblack	1680575	1489	1381
Sauvola	372095	1080	1041
Wolf	372150	1080	1041
Nick	294161	1079	1040
Gatos	319145	1019	1019
Su	152616	1015	1017
Trsingh	369170	1079	1040
Bataineh	491335	1080	1040
Wan	410193	1080	1041
ISauvola	372093	1019	1019
TresholdImage	490780	1018	1019

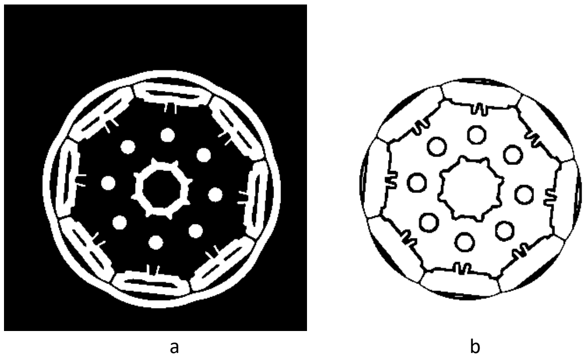

Figure 7. Niblack method (a) and Su method (b).

Table 3. The number of the smudges on Canon's photo.

Binarization methods	Bwareaopen default	Total number of the smudges
Otsu's	21136	21136
Adaptthresh	34382	10862125
Bernsen	1538055	6395664
Niblack	556805	6962227
Sauvola	126840	1394263
Wolf	289595	1184584
Nick	108742	1533448
Gatos	28681	1672989
Su	156732	939738
Trsingh	100972	1421742
Bataineh	10090	18281
Wan	111640	772626
ISauvola	122162	1398941

Table 4. The number of the smudges on Alvium's photo.

Binarization methods	Bwareaopen default	Total number of the smudges
Otsu's	0	0
Adaptthresh	1106132	1112239
Bernsen	5	5
Niblack	1135250	1185880
Sauvola	119765	119767
Wolf	119765	119765
Nick	193687	193703
Gatos	172122	172122
Su	323366	324682
Trsingh	119995	119996
Bataineh	1	1
Wan	87124	87187
ISauvola	119767	119767
TresholdImage	0	0

Table 5. Features of the processed Canon's photo.

Binarization methods	Processed rotor (pixels)	Shades of grey	Width and height
Otsu's	2541663	97	2242 × 2246
Adaptthresh	2763137	143	2243 × 2247
Bernsen	2565473	105	2242 × 2246
Niblack	2574825	108	2243 × 2246
Sauvola	2507434	75	2241 × 2245
Wolf	2502754	71	2241 × 2245
Nick	2501244	69	2241 × 2245
Gatos	2501244	69	2241 × 2245
Su	2498184	66	2241 × 2245
Trsingh	2489576	57	2241 × 2244
Bataineh	2658815	126	2243 × 2247
Wan	2831045	162	2244 × 2249
ISauvola	2507434	75	2241 × 2245
Mean	2572525	107	2242 × 2246

not give good results because there is a large number of pixels in the surface, as with the Niblack method (Figure 7a). The surface of the rotor in the Su method contains the fewest pixels (Figure 7b) for the same reason as in Figure 6b.

For binarized Canon's photo, Table 3 shows the number of pixels removed for each method using the software tool Bwareaopen according to the default settings of the tool. Since it is impossible to remove all smudges with the mentioned tool, pixels that are not part of the rotor surface were removed by the software tools mentioned above. Table 3 shows the total number of removed pixels.

For binarized Alvium's photo, Table 4 shows the number of pixels removed for each method using above explained tools.

The problems that arise when removing smudges from a binarized Canon's photo cannot be seen from the total number of pixels removed from smudges in Table 3. Therefore, the processed photos of the Niblack method (Figure 8a) and the Wolf method (Figure 8b) are shown. In Figure 8a, smudges are still visible that cannot be removed with the tools used. In the processed photo of Figure 8b, it can be seen that there are only 7 holes and that one is missing. The same problem appeared with the Sauvola and Nick methods. In this case, the approximate number of pixels of the rotor was calculated by calculating the number of pixels of existing holes and obtaining their mean value. Depending on how many holes are missing from the processed photo, a certain number of pixels was subtracted in order to obtain an approximate number of pixels of the surface of the processed rotor.

Table 5 shows the pixel counts of the rotor surface from the Canon's photo for each method after the smudges have been removed. The Wan method has the rotor surface with the most pixels, while the Trsingh method has the smallest surface. Their difference gives a deviation of 341469 pixels. Using the algorithm, the threshold shade of grey colour corresponding to the calculated surfaces was calculated, for each method it is shown in Table 5. With the Wan method, the threshold shade is 162 and with Trsingh 57. Table 5 shows the pixel numbers representing the width and height of the processed rotor. With the Adaptthresh, Bernsen and Niblack methods, the width and height decreased significantly after removing the smudges. By calculating the mean value of the number of pixels of the rotor surface of all 13 methods, a surface with a number of pixels of 2572525 pixels is obtained, which corresponds to a shade of grey of 107. Then the photo is binarized according to the calculated mean value of the grey colour shade, smudges are removed and the width containing 2242 pixels and the height with 2246 pixels are calculated Table 5).

In order to visually display the pixels that are within the limits of deviation and their position, each shade of grey colour smaller than 57 and larger than 162 was converted into white colour using the algorithm, while the other shades of grey colour remained unchanged (Figure 9).

Another way to visually display pixels within deviation limits is by using the enlarged view of the left edge (Figure 10). The black colour represents the surface of the rotor, while the shades of grey are the deviation limits.

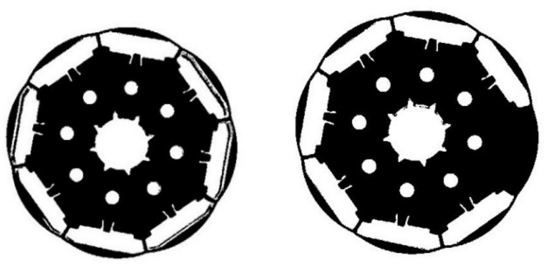

a b

Figure 8. Niblack (a) and Wolf (b) processed photo.

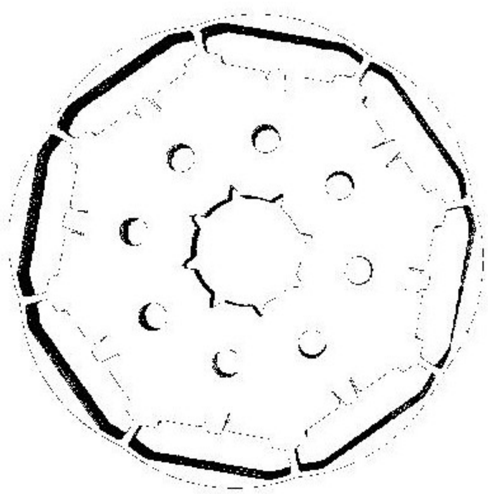

Figure 9. Shades of grey from 57 to 162 for Canon's photo.

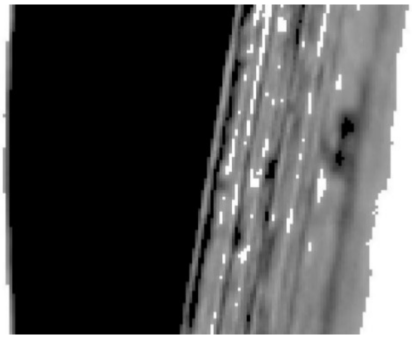

Figure 10. Enlarged view of the rotor with the deviation limits for Canon's photo.

Table 6. Features of the processed Alvium's photo.

Binarization methods	Processed rotor (pixels)	Shades of grey	Width and height
Otsu's	490992	129	1019 × 1020
Adaptthresh	494600	166	1019 × 1020
Bernsen	490780	127	1017 × 1019
Niblack	494695	167	1019 × 1019
Sauvola	491862	138	1019 × 1019
Wolf	491915	138	1019 × 1019
Nick	487864	101	1017 × 1019
Gatos	491267	132	1019 × 1019
Su	477298	41	1015 × 1017
Trsingh	489166	112	1017 × 1019
Bataineh	491334	133	1019 × 1019
Wan	497380	196	1019 × 1019
ISauvola	491860	138	1019 × 1019
TresholdImage	490992	129	1019 × 1020
Mean	490842	127	1017 × 1019

In the Table 6 are the same features like in the Table 5 but for the processed Alvium's photo. It can be seen that the range of shades of grey is much larger, from 41 in the Su method to 196 in the Wan method.

Like in Figure 11 of the Canon's photo on the same way on the Figure 11 of the Alvium's photo are shown Shades of grey from 41 to 196.

On the enlarged view of the rotor of the Alvium photo Figure 12 the limits of deviation of shades of grey are much smaller, i.e. the number of pixels is much smaller than in Figure 10.

To calculate diameter deviation in micrometres, first must be calculated pixel size by dividing the rotor diameter in micrometres by the max mean diameter in pixels [12]. From the Figure 1 rotor diameter is 64.2 mm. Max mean diameter from the Table 5 of the Canon photo is 2246 pixels and from the Table 6 of the Alvium photo is 1019 pixels. The calculation results in a pixel size of 15.23 μm for the Canon's photo, and 33.56 μm for the Alvium's photo. The diameter deviation is finally calculated separately for the width and especially for the height, so that the Max mean diameter is subtracted from these values and multiplied by the pixel size. The obtained results are presented in Table 7.

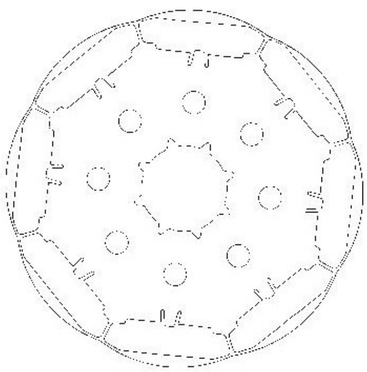

Figure 11. Shades of grey from 41 to 196 for Alvium photo.

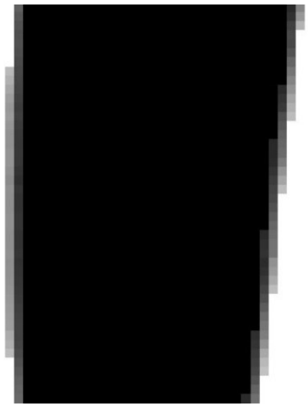

Figure 12. Enlarged view of the rotor with the deviation limits for Alvium's photo.

To use overlay method orientation and centre of the rotor must be same like on "the golden sample". Figure 13 a golden sample (pink) and rotor with same centre but different orientation (green). Black colour shows overlaid pixels of the both samples. When rotating a photo display, it is crucial that the rotor is cut so that it is in the centre of a digital photo that has the same width and height. Table 8 and Table 9 show the coordinates of the centre of the rotor of the processed Canon's

Table 7. Diameter deviation for the processed Canon's and Alvium's photos.

Binarization methods	Diameter deviation for Canon photo (μm)	Diameter deviation for Alvium photo (μm)
Otsu's	– 60.92 + 0	+0 +33.56
Adaptthresh	– 45.69 + 15.23	+0 +33.56
Bernsen	– 60.92 + 0	-67.12 +0
Niblack	– 45.69 + 0	+0 +0
Sauvola	– 76.15 – 15.23	+0 +0
Wolf	– 76.15 – 15.23	+0 +0
Nick	– 76.15 – 15.23	-67.12 +0
Gatos	– 76.15 – 15.23	+0 +0
Su	– 76.15 – 15.23	-134.24 -67.12
Trsingh	– 76.15 – 30.46	-67.12 +0
Bataineh	– 45.69 + 15.23	+0 +0
Wan	– 30.46 + 45.69	+0 +0
ISauvola	– 76.15 – 15.23	+0 +0
TresholdImage	- -	-33.56 +0

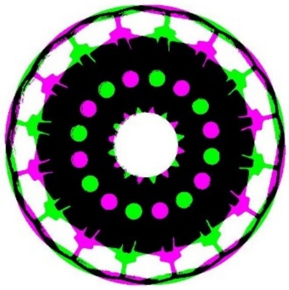

Figure 13. Display of 2 overlaid rotors.

Table 8. Coordinates of the centre of gravity and the centre of the rotor of the processed Canon's photo.

	X	Y
Centre of gravity	2085.4	1796.2
Rotor centre	2086.5	1796.5

Table 9. Coordinates of the centre of gravity and the centre of the rotor of the processed Alvium's photo.

	X	Y
Centre of gravity	841.934	662.741
Rotor centre	841.233	662.547

and Alvium's photos, on the basis of which the centre of the photo is determined. The Canon photo is cropped to dimensions 2261×2261 and Alvium photo on 1051×1051, which is arbitrarily chosen and must be more than the dimensions of the rotor and an odd number. The coordinates of the centre of gravity of the rotor for the Canon and Alvium photo are shown in Table 8 and Table 9, where can see that differ slightly from the coordinates of the centre of the rotor.

With rotation, there is a problem where the pixels are not properly distributed along the edge of the rotor. Figure 14a shows an enlarged part of the rotor that has not been rotated, while Figure 14b shows the same enlarged part of the rotor that has been rotated by 22° clockwise.

In order to analyse the problem that arises in digital photos when rotating the photo of the rotor will be rotated 180° clockwise and vice versa. Then the number of pixels in the surface of the rotor and the number of pixels on the outer edge of the rotor are calculated. Figure 15 and Figure 16 shows the dependence of degrees of rotation on the number of pixels in the rotor surface, while Figure 17 and Figure 18 show the dependence of degrees of rotation on the number of pixels on the outer edge of the rotor.

By analysing Figure 15, Figure 16, Figure 17 and Figure 18, the values of the pixels with the highest value and with the lowest

a b

Figure 14. Non-rotated and rotated part of the photo.

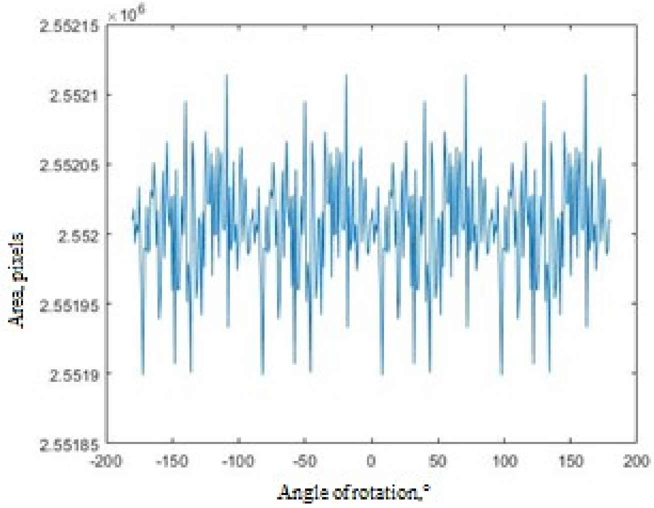

Figure 15. Diagram of the dependence of the number of surface pixels on the angle of rotation for Canon's photo.

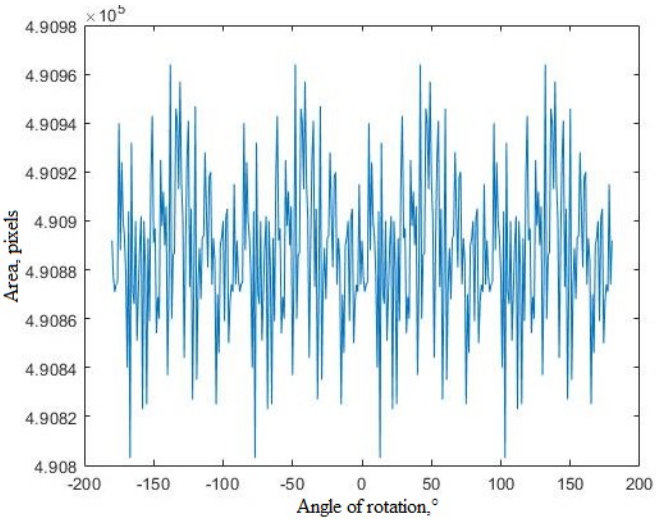

Figure 16. Diagram of the dependence of the number of surface pixels on the angle of rotation for Alvium's photo.

value are determined. The difference between the largest and smallest rotor surface is shown in Table 10 and Table 11, where the first row represents the difference in surface where the angle increased by 0.5 degrees, and the second row is the difference in surface with an increase in angle by 1 degree. The results of the number of edge pixels were analysed in the same way.

Table 10. Maximum deviations of the number of surface and edge pixels during rotation of Canon's photo

Rotation angle, °	Area difference, pixels	Edge difference, pixels
0.5	234	5600
1	215	5479

Table 11. Maximum deviations of the number of surface and edge pixels during rotation of Alvium's photo

Rotation angle, °	Area difference, pixels	Edge difference, pixels
0.5	284	2212
1	161	2211

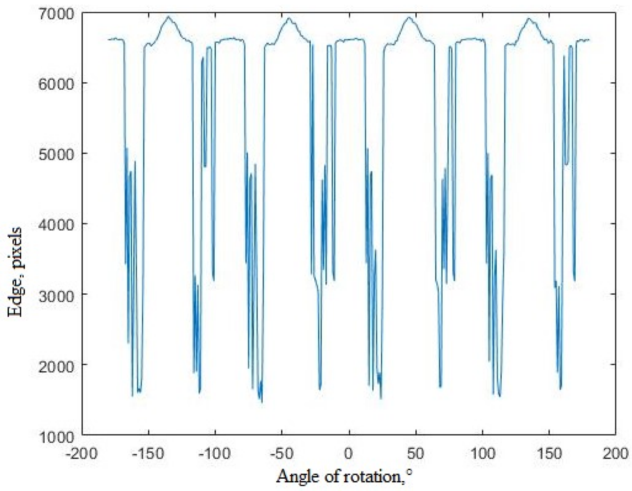

Figure 17. Diagram of the dependence of the number of edge pixels on the angle of rotation for Canon's photo.

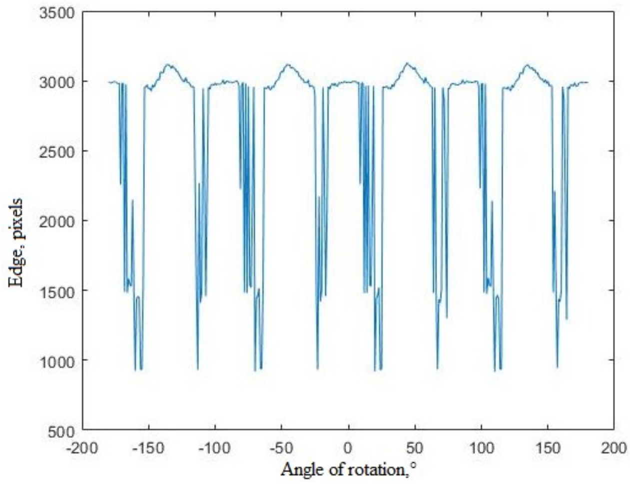

Figure 18. Diagram of the dependence of the number of edge pixels on the angle of rotation for Alvium's photo.

5. CONCLUSIONS

The researched problems arising from the software processing of the digital photograph intended to determine dimensions of the acquired rotor using Canon and Alvium cameras enabled valuable knowledge that will greatly help scientists in this type of research. When binarizing Canon's photo according to the default settings of the tool, there were large deviations in the results of certain methods, which were obvious errors. Methods such as Adaptthresh, Bernsen, and Niblack led to a large increase in the number of pixels because the selected greyscale threshold included a large number of background pixels in the surface of the object. On the other hand, the Sauvola, Wolf, Nick, Gatos, Su, Trsingh and ISauvola methods apparently excluded a large number of pixels from the rotor surface that belong to it.

The main reason for poor results is improperly acquired digital photography because the appearance of shadows or the third-dimension causes problems that cannot be completely removed by software. That problem is partly solved by the equipment from the Figure 4 with recommended features from the paper [12]. On the Alvium's photo is much smaller deviation limit and binarization is better solved. But still the methods Gatos, ISauvola, Nick, Sauvola, Su, Trsingh, Wan and Wolf excluded a large number of pixels. The reason is in default settings of certain methods. With the tool used to remove smudges, in addition to the automatic settings, the settings for the number of pixels of the smudges to be removed are also set. With certain binarization methods, the connected area of smudges is so large that in case of their removal, certain rotor surfaces will also be removed, therefore special algorithms were programmed to avoid the mentioned problem and calculate the surface of the rotor without smudges. The biggest problem occurs with the Canon's photo processed with the Niblack method where a large number of smudges are still visible that cannot be removed because the smudges are connected to the surface of the rotor. Also, with the Nick, Sauvola and Wolf method, there is a problem of removing the holes that are part of the rotor. The reason for this is that the smudges are connected to the hole and were removed by the tools used. Whereby a new problem arises in the case of serial production of a large number of samples and/or using different acquisition devices, the processing of the photo would become time-consuming and complicated because the mentioned algorithm would have to be modified and adapted to the observed photo. With certain methods, in addition to the removal of smudges, it was necessary to add pixels that are part of the rotor and were deleted during binarization. Therefore, in Table 3, the last column shows the total number of smudges that were removed by the Bwareaopen tool and the added smudges calculated by the algorithm. As there are large deviations in the number of pixels of the rotor surface of all methods by Canon's photo, the mean value of the number of pixels of the rotor surface has the largest diameter of the rotor of 2246 pixels (Table 5). This for the actual rotor diameter of 34.2 mm tolerance limits ± 0.04 mm gives a projected pixel size of 15.23 μm which means that the deviation within ± 2 pixels meets the tolerance requirements. Looking at Table 3 and Table 7, it can be concluded that the deviations of the other methods are greater than ± 2 pixels or ± 0.04 mm, which in this case would not meet the tolerance requirements. On the same way for the Alvium's photo, rotor surface with mean value of the pixels has 1019 pixels on the largest diameter (Table 6). Calculated the projected pixel size is 33.56 μm. It means that the deviation within ± 1 pixel meets the tolerance requirements. Bernsen, Nick, Su and Trsingh didn't met tolerance requirements (Table 7). The difference between the method with the most pixels and the method with the fewest pixels within the rotor surface (Table 6) is 20082 pixels, which is 4.1 % of the mean pixel value of all methods, it's much smaller deviation than for the processed rotor on Canon's photo (Table 5) where the deviation is 13.3 %. For the Canon's rotor the largest dimension is 2246 pixels, the photo is cropped on 2261 × 2261 and for Alvium's rotor the largest dimension is 1019 pixels, photo is cropped on 1051 × 1051 so that during rotation the pixels are not lost, which can move and increase in size due to the initial orientation and shape of the rotor. It is also crucial to position the centre of the rotor in the centre of the photo because with most software tools the rotation of the photo display is performed around the centre, otherwise the rotor rotates eccentrically and gives incorrect results when overlapping photos. Which leads to the conclusion that the photo should be cropped to an odd number of pixels in order to be able to determine the central pixel around which the rotation is performed. As the shape of the rotor is symmetrical with slots equally spaced every 45°, it is sufficient to rotate the display only ± 22.5°. When rotating the photo display, it can be concluded that the minimal deviations in the number of pixels are on the surface of the rotor. By rotating by ± 180º, the number of pixels on the surface of the rotor is periodically changed every 90º, which is also the case with the number of edge pixels. While rotation greater than ± 10º results in large deviations in the number of pixels on the edge of the rotor, which creates major problems when the edge is the variable with which dimensional correctness is determined.

As in paper [13], for consideration of certain problems of software photo processing, a photo acquired using a central projection lens was used and the processing was performed using default (automatic) software settings, therefore, this extended research use photography acquired with better quality equipment (Figure 4), a monochrome camera fixed on a stationary tripod, an orthogonal projection lens with a shorter minimum focus length, and illumination under the sample that has parallel light radiation. The processing of the photo acquired with the mentioned equipment gives much better results than the photo acquired with the equipment in Figure 4. Next extended research can be with camera with a larger-sized and higher-resolution sensor as well as other recommended features in the paper [12]. The software tools and their different photo processing settings can be also explored. Since the rotor is circularly symmetrical, it is crucial in future research to program a binarization algorithm that will have the condition that the binarized rotor must have its centre of gravity and centre on the same pixel, as well as the condition that the width and height must have the same number of pixels. On the basis of future research, new valuable knowledge and conclusions would be reached, which will facilitate the software processing of photographs intended for determining the product dimensions and would give better results.

ACKNOWLEDGEMENT

The European Regional Development Fund funded project entitled 'Development of quality control machine and palletizing machine in the automotive industry' (project code: KK.01.2.1.02.0062), within that project was realised this research.

REFERENCES

[1] M. Yang, B. Zhang, J. Zhang, H. Su, Defect detection and classification for mobile phone cover glass based on visual perception, 32nd Chinese Control And Decision Conf. (CCDC), Hefei, China, 22-24 August 2020, pp. 2530-2535. DOI: 10.1109/CCDC49329.2020.9164343

[2] M. Benouis, L. D. Medus, M. Saban, G. Labiak, A. Rosado-Munoz, Food tray sealing fault detection using hyperspectral imaging and PCANet, 21st IFAC World Congress on Automatic Control - Meeting Societal Challenges, IFAC-PapersOnLine, vol. 53, issue 2, 2020, pp. 7845-7850. DOI: 10.1016/j.ifacol.2020.12.1955

[3] G. Ma, Y. Wang, X. Shi, G. Fan, H. Liu , Weld Inspection and Tracking of Laser Welding Head, Laser & Optoelectronics Progress, vol. 55, no. 11, 2018, 111508. DOI: 10.3788/LOP55.111508

[4] J. Sa, Y. An, F. Ye, L. Shi, J. Xu, H. Li, S. Wan, Corrugated Pipe Defect Detection Based on Digital Image Processing, 5th Int. Conf. on Systems and Informatics (ICSAI), Xi'an, China, 25-27 May 2018, pp. 2366-2370. DOI: 10.1109/IMCEC.2018.8469523

[5] N. Chaki, S. H. Shaikh, K. Saeed, Introduction. In: Exploring Image Binarization Techniques. Studies in Computational Intelligence, vol. 560, Springer, New Delhi, 2014, pp. 1-4. DOI: 10.1007/978-81-322-1907-1

[6] R. N. Mitra, S. Mitra, S. Pramanik, B. B. Chaudhuri, A Robust Technique for Delineation and Features Extraction of ECG Signal from Mobile-Phone Photography, Int. Conf. on Communications, Devices and Intelligent Systems (COOlS), Kolkata, India, 28-29 December 2012, pp. 121-124. DOI: 10.1109/CODIS.2012.6422151

[7] C. Zhou, L. Tian, H. Zhao, K. Zhao, A Method of Two-Dimensional Otsu Image Threshold Segmentation Based on Improved Firefly Algorithm, IEEE Int. Conf. on Cyber Technology in Automation, Control, and Intelligent Systems (CYBER), Shenyang, China, 8-12 June 2015, pp. 1420-1424. DOI: 10.1109/CYBER.2015.7288151

[8] S. M. Joseph, P. S. Sathidevi, cDNA Microarray Image Enhancement for Effective Gridding of Spots, IEEE Region 10 Conf. on Technology, Knowledge, and Society (TENCON), Kochi, India, 17-20 October 2019, pp. 326-331. DOI: 10.1109/TENCON.2019.8929512

[9] C. Singh, J. Singh, Multi-channel versus quaternion orthogonal rotation invariant moments for color image representation, Digital Signal Processing, vol. 78, 2018, pp. 376-392. DOI: 10.1016/j.dsp.2018.04.001

[10] K. M. Hosny, M. . M. Darwish, New set of multi-channel orthogonal moments for color image representation and recognition, Pattern Recognition, vol. 88, 2019, pp. 153-173. DOI: 10.1016/j.patcog.2018.11.014

[11] W.-C. Lee, P.-L. Tai, Defect Detection in Striped Images Using a One-Dimensional Median Filter, Appl. Sci. 2020, 10(3), 1012. DOI: 10.3390/app10031012

[12] D. Turinski, I. Svalina, T. Šarić, R. Lujić, S. Havrlišan, Analysis of the problems of acquisition of digital photographs intended to determine the required dimensional accuracy of the product, Int. Conf. on Applied Sciences 2022, Banja Luka, Bosnia and Herzegovina, 24-28-May 2022, J. Phys.: Conf. Ser. 2540 012009. DOI: 10.1088/1742-6596/2540/1/012009

[13] D. Turinski, I. Svalina, T. Šarić, R. Lujić, S. Havrlišan, Problems of software processing of digital photography intended to determining the dimensional accuracy of the product, IMEKO TC11 & TC24 Joint Hybrid Conference, Dubrovnik, Croatia, 17.-19. October 2022. DOI: 10.21014/tc11-2022.04